

**Photoplethysmography based atrial fibrillation detection:  
an updated review from July 2019**

Cheng Ding<sup>\*1,2</sup>, Ran Xiao<sup>\*1</sup>, Weijia Wang<sup>1</sup>, Elizabeth Holdsworth<sup>3</sup>, Xiao Hu<sup>1,2,4</sup>

<sup>1</sup>Nell Hodgson Woodruff School of Nursing, Emory University, Atlanta, GA, USA

<sup>2</sup>The Wallace H. Coulter Department of Biomedical Engineering, Georgia Institute of Technology, Atlanta, GA, USA

<sup>3</sup>Georgia Tech Library, Georgia Institute of Technology, Atlanta, GA, USA

<sup>4</sup>Department of Biomedical Informatics, Emory University School of Medicine, Atlanta, GA, USA

\*These authors contribute equally to this work and share the first authorship.

**Abstract**

Atrial fibrillation (AF) is a prevalent cardiac arrhythmia associated with significant health ramifications, including an elevated susceptibility to ischemic stroke, heart disease, and heightened mortality. Photoplethysmography (PPG) has emerged as a promising technology for continuous AF monitoring for its cost-effectiveness and widespread integration into wearable devices. Our team previously conducted an exhaustive review on PPG-based AF detection before June 2019. However, since then, more advanced technologies have emerged in this field. This paper offers a comprehensive review of the latest advancements in PPG-based AF detection, utilizing digital health and artificial intelligence (AI) solutions, within the timeframe spanning from July 2019 to December 2022. Through extensive exploration of scientific databases, we have identified 59 pertinent studies. Our comprehensive review encompasses an in-depth assessment of the statistical methodologies, traditional machine learning techniques, and deep learning approaches employed in these studies. In addition, we address the challenges encountered in the domain of PPG-based AF detection. Furthermore, we maintain a dedicated website to curate the latest research in this area, with regular updates on a regular basis.

## 1. Introduction

AF is a highly prevalent cardiac arrhythmia, which affects approximately 1-2% of the general population, and is expected to continue to rise in the future worldwide due to population aging [1-3]. Individuals with AF face a substantially heightened risk of experiencing cerebral and cardiovascular complications. Specifically, they are at a fivefold higher risk [4] of ischemic stroke and are associated with an increased risk of ischemic heart disease, sudden cardiac death, and heart failure [5]. In general, people with AF have a four times increased risk of mortality compared to the general population [6]. The current detection of AF heavily relies on routine medical examinations; however, this approach may overlook paroxysmal AF cases, which refer to AF episodes that occur sporadically and self-terminate within 7 days. Additionally, a significant portion of AF patients, estimated at 25% to 35%, remain asymptomatic, which further reduces their likelihood of seeking care. These factors collectively contribute to delays in the identification of AF cases. Consequently, there has been a surge in efforts from both industry and academia sectors for developing technologies that enable reliable and continuous detection of AF. Such technologies are crucial for early identification and timely intervention of AF, which in turn improves patient outcomes.

To enable consistent and long-term monitoring of atrial fibrillation (AF), a solution needs to be non-intrusive, cost-effective, and convenient, reducing operational complexity and encouraging user compliance. To this end, photoplethysmography (PPG) has emerged as a preferred technology, with a ubiquitous adoption in over 71% of wearable devices given its capacity to capture heart rhythm dynamics [7]. The physiological foundation of PPG for AF detection lies in the fact that irregular heartbeats induce variations in cardiac output, leading to fluctuations in peripheral blood volume. This results in irregular pulse-to-pulse intervals and altered morphologies in PPG during AF episodes. Exploiting this physiological basis, wearables equipped with PPG sensors and specialized software offer great promise for personalized self-monitoring

of AF, enabling individuals to receive timely alerts for potential AF episodes. However, the success of this approach hinges on the accuracy of PPG AF detection algorithms. Suboptimal algorithms can easily lead to a surge in false positives, thereby straining healthcare resources through unnecessary or inappropriate medical consultations.

Therefore, it marks tremendous importance for the development of precise and sensitive PPG-based algorithms for AF detection. These algorithms should aim to minimize false detections and optimize the utilization of healthcare resources, ensuring that appropriate clinical guidance is provided to individuals experiencing actual AF episodes. A prior review conducted by Pereira et al. provided a comprehensive summary of research on PPG-based AF detection using statistical analysis, machine learning (ML) and deep learning (DL) approaches up until July 2019 [8]. The review concluded that PPG holds promise as a viable alternative to ECG for AF detection. However, it also highlighted challenges such as the presence of arrhythmias other than AF, motion artifacts in PPG signals from wearable devices, and labor-intensive data annotation processes, among others.

Given the rapid technological advancements in wearable technology and methodological development in artificial intelligence (AI), there is a well-justified need for an updated review of AF detection using PPG. Building upon the previous work by Pereira et al., this paper aims to fill the gap by providing a comprehensive review of the latest developments in utilizing PPG-based digital health and AI solutions for AF detection in both inpatient and outpatient settings from July 2019 to December 2022. The articles included in this review are classified by the three methodological categories established by [8], namely, STAT, ML, and DL, to facilitate the tracking of evolving trends in the field. In addition to conducting a thorough analysis of studies on PPG-based AF detection, this study has established an online knowledge database [9]. This database encompasses all studies reviewed up to December 2022, including those from our work and Pereira's, along with direct links to the respective papers. Committed to keeping the database

current, our team will update it semi-annually. Through the creation of this resource, we aim to foster community collaboration and accelerate the development of effective solutions to this critical clinical challenge.

## 2. Search Criteria

The research team used the SCOPUS, IEEE Xplore, PubMed, Web of Science, and Google Scholar databases to gather appropriate documents for the review. All articles selected were published between July 2019 and up to December 2022, and reviews were eschewed in favor of data-based research studies. Databases function similarly, but not uniformly, so queries needed to be adjusted to reflect this. Filters were used in all databases to restrict the date of publication. Table 1 describes the exact search strings used in different databases for initial document screening. After the documents were retrieved, they were further evaluated for appropriateness for review by two researchers (RX and CD). Based on this search criteria, there are in total 59 studies included in the review, including 17 STAT, 18 ML, and 24 DL studies.

Scientific Database	Search Strings
SCOPUS	(PPG or Photoplethysmography) and (atrial fibrillation or AF or AFib or arrhythmia or cardiac rhythm) and (detection or recognition)
IEEE Xplore	("All Metadata":atrial fibrillation) AND ("All Metadata":wearable computer) AND ("All Metadata:Photoplethysmography OR "All Metadata":PPG)
PubMed	(PPG "OR" Photoplethysmography) "AND" (atrial fibrillation "OR" AF "OR" Afib "OR" arrhythmia of cardiac rhythm) "AND" (detection "OR" recognition)
Web of Science	(PPG or Photoplethysmography)(All Fields) and (atrial fibrillation or AF or afib or arrhythmia or cardiac rhythm)(All Fields) and (detection or recognition)(All Fields)
Google Scholar	(PPG or Photoplethysmography) and (atrial fibrillation or AF or AFib or arrhythmia or cardiac rhythm) and (detection or recognition)

Table 1. Search strings used in different scientific databases for study screening.

## 3. Publication trends in the past decade

Fig. 1 depicts the trends in the number of publications in the three method categories in the past 10 years between January 2013 and December 2022. It reveals an accelerated rate of growth in the number of publications in all three categories, indicating the increasing effort outpouring to developing PPG-based AF detection algorithms. It is worth noting that studies utilizing DL for AF detection emerged in 2017 and expanded rapidly, outpacing the other two categories. In the year 2022, the cumulative number of publications using DL for AF detection exceeded any of the other two categories for the first time in history.

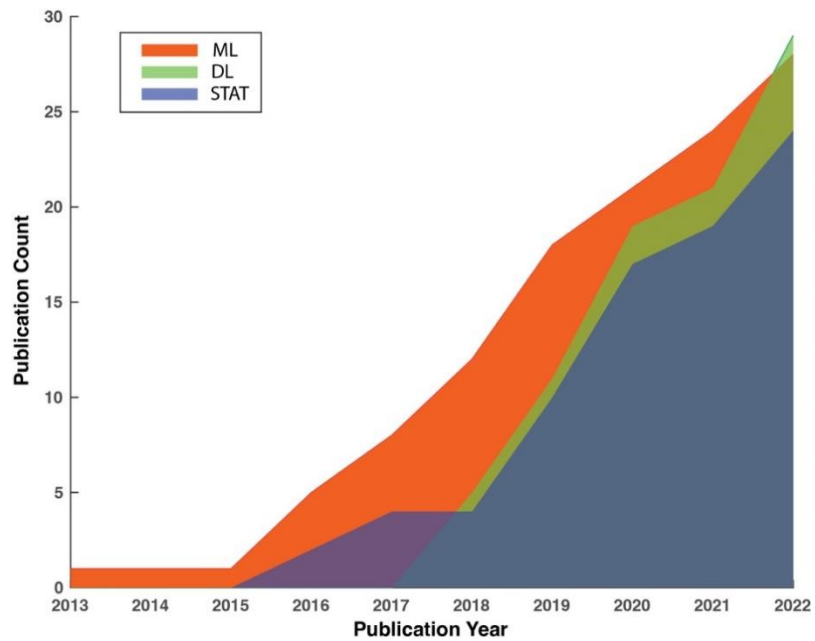


Figure 1. Trends in the number of publications in three method categories using PPG for AF detection.

**Table 2.** Studies on photoplethysmography based AF detection using statistical approaches

Author (year) [ref.]	Number of patients	Dataset features	Age of population	Length PPG segments	Measurement device	Acquisition condition	Input data	Methodology	Performance results for rhythms detection
Väliaho et al. (2019)	213	106 AF, 107 NSR	72.0 ± 14.3 YO	5 min	Wrist band	Outpatient	Pulse-to-pulse interval	Two AF detection algorithms: AF Evidence and COSEn	Sen=0.962; Spe=0.981
Eerikainen et al. (2019)	32	13 continuous AF, 10 non-AF	70 ± 9 YO for continuous AF group, 67 ± 13 YO for AF group	30 sec	Data logger worn on the non-wrist	Outpatient	Inter-pulse interval features: the percentage of inter-val differences of successive intervals greater than 70 ms (pNN70), Shannon Entropy and right wrist based on irregular pulse peak (IPP) and irregular heartbeat (IHB)	Logistic regression	5-min data: Sen=0.989; Spe=0.990; Acc=0.990; 24-hour data: Sen=0.970; Spe = 0.920; Acc = 93.91%  Patient-level performance by IPP: 15%; Sen=0.970; Spe=1; PPV=1; NPV=0.970
Kabutoya et al. (2019)	59	29 AF, 30 NSR	66.5 ± 12.2 YO for AF group, 67.7 ± 8.0 YO for NSR group	25 sec	Wrist monitor	Outpatient	3 measurements for the left and right wrist based on irregular pulse peak (IPP) and irregular heartbeat (IHB)	Detection rule: "monitor AF in irregular pulse peak (IPP) 15/20/25" defined as follows: (a) IPP: interval of pulse wave – the average of the interval of the pulse wave ≥ the average of the interval of the pulse wave × 15/20/25%; (b) irregular heartbeat (IHB): beats of IPP ≥ total pulse × 20%; and (c) the " monitor AF (IPP 15/20/25)" : ≥ 4 IHBs	
Bashar et al. (2019)	UMass database 37, Chon Lab database 9	UMass database: 10 AF and 27 non-AF; Chon Lab database: 9 healthy	--	30 sec	Wrist and watch	Outpatient	Root mean square of successive differences (RMSSD) and sample entropy (SampEn) from the pulse intervals	Weighted average of two features and threshold-based rule	Sen=0.982, Spe=0.974 Acc=0.975
Bashar et al. (2019)	20	8 AF, 12 non-AF	--	30 sec	Wrist watch	Outpatient	Root mean square of successive differences (RMSSD) and sample entropy (SampEn) from the pulse intervals	Weighted average of two features and threshold-based rule	Sen=0.962 Spe=0.974 Acc=0.971
Han et al. (2019)	16	Patients: 11 NSR and 3 with PAC/PVC, 2 with basal heart rate AF and 3 with fast AF	63-88 YO	30 sec	Smart watch	Outpatient	Not an Afib deletion study but the HR estimation study using ppg	--	--
Sološenko et al. (2019)	34	Clinical testing database with 15 AF and 19 non-AF, plus two simulated developmental and testing databases	Clinical testing database 72.9 ± 8.9 YO for AF group, 67.5 ± 10 YO for non-AF group	30 sec	PPG simulator	Simulation	PP or RR interval	Threshold based detector using Heaviside step function to calculate sample-entropy like index	Two sets of performance based on different signal quality thresholding of the dataset, sensitivity of 72.00% and a specificity of 99.70% when 89.20% of the database ; 97.20% and a specificity of 99.60% were achieved when increasing the
Han et al. (2020)	37	All patients have cardiac arrhythmia	50-91 YO	30 sec	Wrist watch	Outpatient	This is for PAC/PVC detector for AF patients or NSR subject, not for detecting AF	--	--
Inui et al. (2020)	40	Patients scheduled for cardiac surgery	Mean (SD) 70.9 YO (11.1)	1min	Smart watch and wrist band	Outpatient	This is for using ppg for pulse rate estimation in AF as compared to ECG	--	--

**Table 2.** Studies on photoplethysmography based AF detection using statistical approaches

Author (year) [ref.]	Number of patients	Dataset features	Age of population	Length PPG segments	Measurement device	Acquisition conditions	Input data	Methodology	Performance results for rhythms detection
Estrella-Gallego et al. (2020)	9	4 AF, 9 Non-AF	35-80 YO	30 sec	Smartphone	Outpatient-continuous measurement	PPG signals with Offset removed and EWMA filter applied for smoothing	--	--
Válleho et al. (2021)	359	169 AF, 190 NSR	72.2 ± 14.3 YO for AF	1 min	Wrist band	Inpatient-checkpoint	The five pulse interval-based variables were: mean PIN, root-mean-square values of successive	Linear logistic regression	Sen=0.964 Spe=0.963 AUC=0.993
Avram et al. (2021)	204	32 no history of AF, 159 paroxysmal AF, 16 with persistent AF	62.6 ± 11.6 YO	5 min	Smartwatch	Outpatient-continuous measurement	IBI features: the dispersion of the Poincaré plot, the standard deviation and the modified Shannon entropy	Logistic regression model	Sen=0.878 (95% confidence interval [CI] 0.836–0.910) Spe=0.974 (95% CI 97.10%–97.70%)
Chorin et al. (2021)	18	6 AF, DM 4 HTN 8, Brugada syndrome 3, DFT after ICD implant 5	59.4 ± 21.3 YO	1 min	Cardiac Sense Smartwatch	Outpatient-continuous measurement	RR and GG intervals of PPG and ECG	Threshold based defibrillation	
Chang et al. (2022)	200	112 AF, 88 non-AF	66.1 ± 12.6 YO	5 min	Garmin smartwatch	Outpatient-continuous measurement	Standard deviation of normal-to-normal intervals and root mean square of successive RR interval	An undisclosed heart rate classifier	Performance based on 5-min segments: Sen=0.971, Spe=0.868 PPV of AF detector=0.897
Han et al. (2022)	35	23 NSR, 5 PAC/PVC, 5 Basal AF, 5 AF with RVR	50 to 91 YO	30 sec	Smartwatch	Outpatient-continuous measurement	Root mean square of successive differences (RMSSD) and sample entropy (SampEn) from the pulse intervals	Weighted average of two features and threshold-based rule	Not reported, AF detection is a part of the procedure for estimating HR.
Válleho et al. (2022)	173	76 AF, 97 NSR	AF: 77.1 ± 9.7 YO, NSR: 67.3 ± 15.1 YO	1 min	Wrist band	Outpatient-continuous measurement	The five-pulse interval-based variables were: mean PIN, root-mean-square values of successive differences (RMSSD), AF Evidence (AFE), Coefficient of	Linear logistic regression	30-min time-frame performance: Sen=0.947, Spe=0.969 F1=0.954
Nonoguchi et al. (2022)	286	163 with high AF risk, 123 with known AF	66 ± 12 YO for high-risk group, 67 ± 12 YO	30 min	Wristwatch-type continuous pulse wave monitor	Outpatient-continuous measurement	Features based on pulse period (PP) values: CV, degree of variation and KS, Kolmogorov-Smirnov difference.	A rule-based algorithm using CV and KS	Patient-level performance: Sen=0.980 Spe=0.906 PPV=0.694 NPV=0.995, Interval level performance: 0.869, 0.988, 0.896, and 0.985

Table 3 Studies on photoplethysmography based AF detection using ML approaches

Author (year) [ref.]	Number of patients	Dataset features	Age of population	Length PPG segment s	Measurement device	Acquisition conditions	Input data	Methodology	Performance results for rhythms detection
Yang et al. (2019)	11	Patients referred to hospital in AF state	63 ± 12 YO	5, 10, 15, 20 sec	Customized wrist-type device	Inpatient	Statistical measures of Wavelet transform coefficients (mean, median, standard deviation, variance, Shannon entropy, energy, contrast, inverse different moment, homogeneity) Time series features: crest to crest intervals, trough to trough intervals, heart rate.	Support Vector Machines with polynomial and radial-basis function kernels Artificial neural network (ANN), support vector machine (SVM), Logistic regression, decision trees and Bagging decision trees	Sen=0.701; Spe=0.886; Acc=0.804  Sen=0.980; Acc=0.977
Neha et al. (2019)	15	13 PPG records for training and 2 PPG sample for testing (MIMIC II)	-	24 sec	Finger pulse from bedside monitors	Inpatient	PPG-wave features: Adaptive organization index (AOI); Variance of the slope of the phase difference (VSPD); Permutation entropy (PE); Spectral entropy (SE); Fractional spectral radius (FSR); Spectral purity index (SPI); RR time series features: mean, standard deviation, median, Interquartile range, Minimum, Peak-to-peak intervals of ppg for uniform SR, the variance, entropy derived from the peak-to-peak intervals were fluctuating for AF episodes	Support Vector Machines with polynomial and radial-basis function kernels Artificial neural network (ANN), support vector machine (SVM), Logistic regression, decision trees and Bagging decision trees	AF vs NSR: Sen=0.997; Spe=0.924; Acc=0.981; PPV=0.979; NPV=0.989; F1=0.990. AF vs (SR&VA): Sen=0.962; Spe=0.928; Acc=0.950; PPV=0.959; Sen=0.93; Spe=0.84; PPV=0.85
Fallet et al. (2019)	17	All patients referred for catheter ablation of cardiac arrhythmia (415 epochs of ventricular arrhythmia (VA), 1370 samples of AF and 381 424 suspected AF, 227 confirmed AF	57 ± 13 YO	10 sec	Wrist-type device	Inpatient-continuous measurement	Peak to Peak intervals of PPG, Kolmogorov-Smirnov test for normality of continuous variables, Normal distributions presented as Mean (SD), Mann-Whitney Test values for categorical values.	Boosting Algorithm	Sen=0.955; Spe=0.991; PPV=0.931; NPV=1; Kappa=0.960.
Guo et al. (2019)	224	20 AF, 140 NSR, Hypertension 47, diabetes 23, artery disease 14, current smoking 24 and	Mean age 53 YO	45 sec	Wrist-type device	Inpatient-continuous measurement	Mean IBI; standard deviation of IBI; SDSD (standard deviation of the successive differences between IBI); pSD50 (percentage of successive differences between IBI greater than 50 ms)	K Nearest Neighbors (KNN); Support Vector Machine with linear kernel (Linear SVM); Support Vector Machine with radial basis function kernel (RBF SVM); Decision Trees (DT); Linear SVM	Best performance: RBF-SVM. Sen, Spe and Acc= over 0.975 (specific performance unavailable due to graphic presentation); F1=0.985
Zhang et al. (2019)	375	100 AF, 100 NSR	-	20, 30, 40, 50, 100, 150, 200, 250 and 300	PPG simulator based on phenomenological model	-	Variability analysis of IBI time series: mean, standard deviation, root of the mean squared differences of successive intervals, (RMSSD), the percentage of interval differences of successive intervals greater than x rms (pNNx, with x = [20, 50, 70]), irregularity of IBI	Random Forest	Signal length (20-300 beats): Sen=0.881-0.991; Spe=0.940-1; Acc=0.913-0.995.
Buś et al. (2020)	32	8 NSR recordings (total length of 240 min), 24 AF recordings (total length of 120 min); 253 AF samples; 381 NSR samples	-	32 consecutive inter-beat interval (IBI)	Finger pulse wave acquisition system Portapres 2 (FNS, Holland)	Outpatient-continuous measurement	IBI features: Shannon Entropy (ShEn); Normalized Root Mean Square of Successive Differences r (nRMSSD); pNN40 and pNN70; Sample Entropy (sampEn); Coefficient of Sample Entropy (CoSEn); PPG waveform features: Kurtosis; Hjorth mobility; Hjorth variability parameters; peak amplitude; and other signal characteristics	Support Vector Machine with radial basis function kernel (RBF SVM); Decision Trees (DT); Linear SVM	AF vs AFL vs Other: Sen=0.9760, 0.845/0.981; Spe=0.9820, 0.9770, 0.928; Acc=0.98170, 0.9640, 0.966.
Corino et al. (2020)	200 simulated PPG signals	276 hours of AF, 116 hours of atrial flutter (AFL), and 472 hours of other rhythms (NSR, and sinus rhythm	Mean age in training set: 66 YO in AF, 63 YO in AFL and 69 YO in Other;	30 sec	Wrist-type data logging device equipped with the Philips Cardio and Motion Monitoring Smartphone,	Inpatient	Several rhythm and signal features, such as heart rate variability parameters, peak amplitude, and other signal characteristics	SVM	AF vs NSR: Sen=0.963; Spe=0.935; Acc=0.949
Enrikäinen et al. (2020)	40	828 NSR signals and 828 AF signals from five open Physionet datasets	-	-	Finger pulse from bedside monitors	Inpatient-continuous measurement	IBI time series features: Mean, standard deviation (STD), median absolute deviation (MAD), root mean square of successive differences (RMSSD), the standard deviation of Poincaré plot perpendicular to the line-of-identity (SD1), the standard deviation of R-R intervals (SDRR), total heart rate variability (S). Time-frequency domain features: mean absolute value of approximation coefficients (MAV(A)), average energy of approximation coefficients (AEC(A)), standard deviation of approximation coefficients (STD(A))	XGBoost	AF vs NSR: Sen=0.984; Spe=0.995; Acc=0.990



Table 3. Studies on photoplethysmography based AF detection using ML approaches.

Author (year) [ref.]	Number	Dataset features	Age of population	Length PPG segments	Measurement device	Acquisition conditions	Input data	Methodology	Performance results for rhythms detection
Aydemir et al. (2020)	7	subject's signals acquired in squat, stepper and resting phase	20 to 52 YO	3-sec window-length PPG segments for 48 sec	Wrist bracelet	-	Mean, standard deviation, autoregressive model parameter, values of the real part and standard deviation, values of the imaginary part	K-nearest Neighbor, Bayes, and Decision Tree	Acc=0.930, C.A rate= 0.890
Guo et al. (2021)	604	Individuals at high risk for AF.	More than 18 YO	48 sec	Huawei smart device and Hollar ECG	Outpatient-continuous measurement	1) Heart rate: minimum value of all RR intervals (MinHR), mean value of all RR intervals (MeanHR), and skewness of all RR intervals (SKRR); 2) heart rate variability: coefficient of variation of all RR intervals (CVRR), standard deviation of all RR intervals (SDRR)	XGBoost	AF vs NSR: Sen=0.821; Spe=0.974; Acc=0.935; PPV=0.914; F1=0.865; AUC=0.971
Xie et al. (2021)	21	Healthy participants	--	10 sec	Wearables on forearm	Outpatient-checkpoint	Wavelet transform based features	SVM	AF vs NSR: Acc=0.983
Neha et al. (2022)	53	Prospective Data: 15 PVC, 15 sinus tachycardia, 15 NSR, and 8 AFL. Retrospective Data: 7 premature ventricular contractions, 6 sinus tachycardia, 15 DC cardioversion of AF to NSR, 29 patients exhibit various arrhythmias including AF, and 13 patients scheduled for cardiovascular surgery	59.93 YO for PVC, 44.13 YO for sinus tachycardia, 59.93 YO for NSR, 54.87 YO for AFL	16 sec divided to 2 segments of 8 sec	Polar OH1 optical sensor	Inpatient	The Poincare Plot dispersion, the modified Shannon entropy, the sample standard deviation, the sample mean, the mean stepping increment, the kurtosis, and the skew.	Hybrid Decision model with logistic regression and a heuristic statistical decision model based on Shannon Gradient Boosting Decision Tree	AF vs NSR: Sen=0.878; Spe=0.974.
Zhu et al. (2022)	70	28 patients undergo elective DC cardioversion of AF to NSR, 42 patients scheduled for cardiovascular surgery	69.3±10.9 YO for the 28 patients and 35.4 ± 5.7 YO for the 42 participants	5min	Samsung smartwatch	Outpatient-continuous measurement	Median value of the mean and SD of PPG pulse rate	Random Forest	AF vs NSR: Sen=0.941; Spe=0.934; Acc=0.937; PPV=0.930; and NPV=0.939
Hiraoka et al. (2022)	80	Patients with paroxysmal AF, 40 patients with persistent AF	Mean (SD) 65.8 (13.4) YO excluding one	10 min	Apple watch	Inpatient-continuous measurement	IBI time series features: Shannon entropy (ShEn), normalized root mean square of successive differences (nRMSSD), percentage of differences of successive IBI that exceed 40 or 70 ms (pNN40, pNN70), sample entropy (sampEn) and coefficients of sample entropy (CoSEn) of embedding dimensions 1 and 2, turning point ratio (TPR), minimum, maximum, mean and standard deviation (std) of IBI time series	Ridge regression, random forest, K-Nearest Neighbors and SVM	AF vs non-AF vs NSR: average Sen=0.734; Spe=0.879; Acc=0.840; PPV=0.645; NPV=0.841
Liao et al. (2022)	116	76 patients with paroxysmal AF, 40 patients with persistent AF	59.6 ± 11.4 YO	10, 25, 40, and 80 heartbeats	Wrist worn smartwatch	Outpatient-continuous measurement	Frequency domain features: Horith mobility and complexity, spectral entropy (specEn) and spectral purity index (SPI) pulse wave analysis (PWA) features: pulse foot, the systolic raise, the anacrotic notch (AN), the post-AN systolic peak, the dicrotic notch and the diastolic peak	Ridge regression, random forest, K-Nearest Neighbors and SVM	AF vs NSR: Sen=0.821; Spe=0.974; Acc=0.935; PPV=0.914; F1=0.865; AUC=0.971
Jeaningros et al. (2022)	42	42 patients referred for catheter ablation	--	30 sec	Wrist bracelet	Outpatient-continuous measurement	IBI time series features: Shannon entropy (ShEn), normalized root mean square of successive differences (nRMSSD), percentage of differences of successive IBI that exceed 40 or 70 ms (pNN40, pNN70), sample entropy (sampEn) and coefficients of sample entropy (CoSEn) of embedding dimensions 1 and 2, turning point ratio (TPR), minimum, maximum, mean and standard deviation (std) of IBI time series	Ridge regression, random forest, K-Nearest Neighbors and SVM	AF vs non-AF vs NSR: average Sen=0.734; Spe=0.879; Acc=0.840; PPV=0.645; NPV=0.841

**Table 2.** Studies on photoplethysmography based AF detection using DL approaches

Author (year) [ref.]	Number of patients	Dataset features	Length PPG segments	Measurement device	Acquisition conditions	Methodology	Performance results for rhythms detection
Shen et al. (2019)	29+53	13 with persistent AF, 2 with NSR, and 14 with changed rhythm, additional 53 healthy	30 sec	Samsung wrist-wearable device	Outpatient--continuous measurement	1D ResNeXt	0.950
Yousefi et al. (2019)	30	15 with AF, 15 with NSR	30 consecutive PPG pulses	Wrist-worn PPG monitor	Inpatient	Deep NN	All data: Sen=0.936 ± 0.216 Spe=0.992 ± 0.180 AUC=0.996 After quality assessment: Sen=99.2± 1.3
Zaen et al. (2019)	105	84 from Long-Term AF Database from PhysioNet, 21 from University of Alabama	30 sec	Tri-axis accelerometer	Outpatient--continuous measurement	RNN	Without outlier rejection: Acc=0.929 Sen=0.980 Spe=0.912 F1=0.875 With outlier rejection: Acc=0.986 Sen=1 Spe=0.978 F1=0.964
Kwon et al. (2019)	75	57 for persistent AF, 18 for long-standing persistent AF/underwent successful	30 sec	Pulse oximeter	Outpatient--checkpoint	1D CNN	Sen=0.993 Spe=0.959 Acc=0.976 PPV=0.960 NPV=0.993 AUC=0.998
Neha et al. (2019)	15	13 samples for training, 2 samples for testing	24 sec	PPG based sensors	Inpatient	Deep NN	Precision 0.960 Recall 0.950 Acc=0.954 F1=0.950
Aschbacher et al. (2020)	51	All patients with persistent AF/Patients undergoing electrical cardioversion were	10 sec	Smartwatch	Outpatient--continuous measurement	LSTM/ CNN	LSTM 0.954 Sen=0.810 Spe=0.921 DCNN Sen=0.985 Spe=0.880 AUC=0.983
Torres-Soto and Ashly (2020)	163	107 for cardioversion group, 41 for exercise stress test group, and 15 for ambulatory	25 sec	Did not specify	Outpatient--continuous measurement	Autoencoder+1DCNN	Sen=0.980 Spe=0.99 F1=0.960 FPR=0.01 FNR=0.02
Seider et al. (2020)	60	AF was identified in 6 (10%) subjects, of which 4 were previously undiagnosed	60 sec	Wristband	Outpatient--continuous measurement	LSTM for quality assessment, Tree based classifier for AF detection	Sen=1 Spe=0.960 ACC=0.970 NPV=1 PPV=0.750
Aschbacher et al. (2020)	51 + 13	40 for algorithms training, 11 for algorithms testing/ 51 patients were enrolled	Roughly 30 seconds	Wrist-worn fitness tracker	Inpatient	Model1: Logistic regression Model2: LSTM Model 3: DCNN	Model 1: Sen=0.741 Spe=0.584 AUC=0.717 PPV=0.808 NPV=0.488 Model2: Sen=0.810 Spe=0.921 AUC=0.954 PPV=0.960 NPV=0.671 Model3: Sen=1 Spe=0.966 Acc=0.979
Genzoni et al. (2020)	37	All patients are for catheter ablation procedures and wear an optical heart rate monitor device	30 sec	Wrist-worn device	Outpatient--continuous measurement/ inpatient	GRU	

Table 2. Studies on photoplethysmography based AF detection using DL approaches

Author (year) [ref.]	Number of patients	Dataset features	Age of population	Length PPG segments	Measurement device	Acquisition conditions	Input data	Methodology	Performance results for rhythms detection
Chen et al. (2020)	401	All patients had a stable heart rhythm	>18 YO	71 sec	Wristband	Inpatient and outpatient--checkpoint	PPG segment	SEResNet	Sen=0.950 Sep=0.990 Acc=0.976 PPV=0.986 NPV=0.970
Kwon et al. (2020)	100	81 for Persistent AF, 19 for long-standing persistent AF	≥20 YO	30 sec	Ring-type wearable device	Outpatient--checkpoint	PPG segment	1D CNN	Sen=0.990 Spe=0.943 Acc=0.969 PPV=0.956 NPV=0.987 AUC=0.993
Aschbacher et al. (2020)	51	All patients with persistent AF/Patients undergoing electrical cardioversion were sedated and remained supine	63.6±11.3 YO	10 sec	Smartwatch	Outpatient--continuous measurement	PPG segment	LSTM/ CNN	LSTML 0.954 Sen=0.810 Spe=0.921 DCNN Sen=0.985 Spe=0.880 AUC=0.983
Cheng et al. (2020)	MIMIC-III waveform database: 30000 patients, IEEE	60 sick subjects from MIMIC-III, 42 patients from IEEE TBME and 15h of PPG from synthetic dataset	TBME Respiratory Rate Benchmark data set: children	10 sec	ICU monitor and pulse oximeter	Inpatient and outpatient--continuous measurement	time-frequency chromatograph	CNN-LSTM	Sen=0.980 Spe=0.981 Acc=0.982 AUC=0.996
Ramesh et al. (2021)	37	10 with AF, 27 non-AF	--	30 sec	Simband	Outpatient--continuous measurement	Time domain features	CNN	Sen=0.946±0.02 Spe=0.952±0.07 Acc=0.951±0.03F1=0.893±0.
Zhang et al. (2021)	53	38 for NSR, 5 for persistent AF and 10 for nonventricular AF	66.3 ± 11.8 YO	30 sec	Smartwatch	Outpatient--continuous measurement	PPG segment	multi-view convolutional neural network	Ave of Acc=0.916 Spe=0.930 Sen=0.908
Das et al. (2022)	175	108 with AF, 67 non-AF	--	25 sec	Wrist-worn wearable device	Outpatient--continuous measurement	PPG segment	Bayesian deep neural network	Without uncertainty threshold: Sen=0.722 Spe=0.720 Precision 0.627 F1=0.671 AUC=0.793 Without threshold.
Ding et al. (2022)	139	126 for UCLA medical center, 13 for UCSF Neuro ICU	18-95 YO for UCLA medical center, 19-91 YO	30 sec	Pulse oximeter	Inpatient--continuous measurement	PPG segment	ResNet	Sen=0.928 Sep=0.988 Acc=0.961 PPV=0.985 NPV=0.943
Sabbadin et al. (2022)	4158 /88	56 from MIMIC database (13 AF), 32 from UQVSD database (2 AF)	--	10 sec	PPG device (did not find specified device name?)	Outpatient--continuous measurement	Root-Mean-Square (RMS) and the mean of Skewness and Kurtosis	Deep NN	F1=0.920 Precision 0.890 Recall 0.950

**Table 2.** Studies on photoplethysmography based AF detection using DL approaches

Author (year) [ref.]	Number of patients	Dataset features	Age of population	Length PPG segment	Measurement device	Acquisition conditions	Input data	Methodology	Performance results for rhythms detection
Nguyen et al. (2022)	40	18 with NSR, 15 with AF, and 7 with PAC/PVC	--	30 sec	PPG sensor patch measured	Outpatient--checkpoint	poincare plot	2D CNN	Sen=0.968 Spe=0.989 Acc=0.981
Liu et al. (2022)	228	Patients all have arrhythmia	52.3±11.3 YO	10 sec	Fingertip PPG sensor	Outpatient--continuous measurement	PPG segment	1D CNN	AF Spe=0.934 Acc=0.944 PPV=0.890 NPV=0.940
Neha et al. (2022)	670 PPG signals /23	400 normal, 90 PVC, 90 tachycardia, and 90 atrial flutters	--	8 sec	ICU monitor	Inpatient	Dynamic time warping based features	Deep NN	Sen=0.970 Spe=0.970 Acc=0.960 F1=0.960 precision=0.960
Ding et al. (2022)	28539 patients, UCSF HER dataset, IUCVA	Female AF 2304, Male AF 3473, Female cohort 13203, Male cohort 15330, NSR, PVC	22 to 65 YO	30 sec	Fingerprint, Wearable device	--	PPG segment	Autoencoders + ResNet	AUC=0.960
Kwon et al. (2022)	35	All patients underwent successful electrical cardioversion for AF	Mean 58.9 YO	10 sec	Smart wriing	Outpatient--continuous measurement	PPG segment	Not specify	AUROC 0.995 Sen=0.987 Spe=0.978 FPR=0.02 FNR=0.01

## **4. Review of recent studies on PPG-based AF detection**

### **4.1 Updates on PPG-based AF detection using statistical analysis approaches**

A compilation of studies for PPG-based AF detection employing statistical analysis approaches is summarized in Table 2. The table provides an overview of these studies in chronological order, including patient cohorts, data characteristics, employed features and methods, care settings (inpatient versus outpatient), and the resultant performance outcomes. It shows that the statistical analysis approach mainly relies on threshold-based rules on the selected set of features for AF detection. Under this umbrella, the most frequently employed features for AF detection include the RR interval from the ECG and the inter-beat interval (IBI) from PPG [10-15]. Additionally, the root mean square of successive differences (RMSSD) and sample entropy (SampEn) are also among the most utilized features [16-20]. Consequently, the extracted features undergo analysis in terms of their histograms, both with and without the presence of AF and other cardiac rhythms. This analysis assists in determining optimal thresholds that effectively differentiate various rhythmic classes. Once these thresholds are established, they can be applied to the same features extracted from PPG signals.

Furthermore, the utilization of identical feature sets with alternative statistical approaches, such as logistic regression, enhances the versatility and comprehensiveness of AF detection studies. By applying logistic regression, researchers can establish a mathematical model that estimates the probability of AF presence based on the input features. The logistic function, also known as the sigmoid function, is employed to transform the output into a range between 0 and 1. This transformed probability serves as an indicator of the likelihood of AF compared to non-AF cases. The advantage of logistic regression lies in its ability to provide a quantitative measure of the probability, allowing for a nuanced understanding of the classification outcome. Also, as reported in Table 2, studies incorporating larger patient cohorts intend to utilize logistic regression [14, 16, 19] rather than rule-based models. This observation aligns with the trends identified in a previous

review study [8], further reinforcing the preference for logistic regression in cases involving a higher number of patients.

As compared to the previous review, we observe a rising number of studies using the statistical analysis approach (4.25 studies/year between 2019 and 2022 vs. 2 studies/year between 2013~2019), which aligns with the rising number of all-type AF detection studies in recent years. It can be observed that more studies focus on outpatient populations, which might be attributed to the rapid advancement of wearable technology in recent years.

#### **4. 2 Updates on PPG-based AF detection using machine learning approaches**

Table 3 presents a chronological summary of AF detection studies based on machine learning approaches in the last four years. Machine learning has demonstrated promising results in the detection of AF in low-sample settings. The application of ML techniques requires domain expertise for feature engineering to extract features that effectively capture the comprehensive characteristics of PPG waveforms and enable the discrimination of different classes. Commonly extracted features include morphological descriptors, time domain statistics, statistic measurements in the frequency domain, nonlinear measures, wavelet-based measures, and cross-correlation measures.

Of different machine learning algorithms, Tree-based algorithms, such as Decision Trees, Random Forest, and Extreme Gradient Boosting (XGBoost) [21], are the most popular choices and are collectively employed in 12 out of the 18 studies employing machine learning for AF detection. Random Forests have demonstrated strong performance in AF detection tasks using PPG. This ensemble learning algorithm combines multiple decision trees to create a robust classification model. By aggregating the predictions of individual trees, Random Forests can reduce overfitting, handle complex feature interactions, and provide accurate AF detection results. The versatility, interpretability, and resilience to noisy data make Random Forests a popular choice in PPG-AF detection research. XGBoost is a boosting algorithm that combines gradient

boosting with decision trees to achieve high predictive accuracy in PPG-AF detection. XGBoost sequentially builds an ensemble of weak models, iteratively improving its performance by minimizing a loss function. It can effectively handle complex feature interactions and capture subtle patterns in PPG signals, leading to improved AF classification results and better detection performance compared to individual decision trees.

The second most popular (used in 8 out of 18 studies) machine learning classifier for AF detection is Support Vector Machines (SVM) [22], due to their ability to handle high-dimensional feature spaces. SVM separates PPG signal data into different classes by identifying an optimal hyperplane that maximizes the margin between the classes. By mapping PPG signals into a higher-dimensional space, SVM can capture complex relationships and find effective decision boundaries for accurate AF classification. There are also other classifiers adopted in the studies such as K-Nearest Neighbors (KNN) and artificial neural networks (ANN) but are not widely adopted as the above two classifiers.

Compared to the previous review, we observe a sharp increase in the adoption of machine learning for AF detection using PPG (5 studies/year between 2019 and 2022 vs. 1.5 studies/year between 2016 and 2019).

### **4.3 Updates on PPG-based AF detection using deep learning approaches**

Deep learning has emerged as a powerful approach for detecting AF in PPG signals, as reported in Table 4. Unlike traditional ML methods, DL models can learn comprehensive feature representations through an end-to-end learning fashion, eliminating the need for complex feature engineering. This is achieved by learning from a large amount of training samples to train deep neural networks, which consist of interconnected layers of computational nodes.

As shown in Table 4, studies using DL approaches can be divided into two main categories. The first category (employed in 14 out of 24 studies) is a family of convolutional neural networks (CNN).

CNN is commonly applied in computer vision tasks, but they have also been successfully adapted for PPG-AF detection. CNNs utilize convolutional layers to automatically extract relevant features from the PPG signal data [23]. These convolutional layers apply numerous filters across the signal, allowing the network to capture local patterns and identify important discriminative features associated with AF. By stacking multiple layers, CNNs can learn increasingly complex representations of the PPG signals, enhancing the accuracy of AF detection. Residual network (ResNet) [24], a specific type of CNN, addresses the challenge of training deep neural networks by utilizing skip connections. These connections allow the network to bypass layers and pass information directly to subsequent layers, mitigating the vanishing gradient problem. In the context of PPG-AF detection, ResNet architectures enable the training of deeper networks with improved performance and ease of optimization. By incorporating residual connections, ResNet models can capture fine-grained details and long-range dependencies in PPG signals, leading to enhanced AF detection capabilities. The second category is a family of sequential DL models, of which Long Short-Term Memory ( LSTM ) [25], is a popular choice (employed in 4 out of 24 studies). LSTM is a recurrent neural network architecture commonly used in PPG-AF detection due to its ability to effectively capture temporal dependencies in sequential data. In the context of PPG signals, LSTM models can analyze the sequential nature of the data, considering the temporal order of the signal samples. This allows LSTM to capture long-term patterns and dynamic changes in the PPG signals, which are crucial for accurate AF detection.

To effectively train DL models, a substantial amount of labeled training data is typically required. However, in biomedical applications, the availability of labeled data is often limited. Transfer learning is a potential solution to this challenge, wherein a pre-trained DL model is fine-tuned for a specific task. The number of layers and the complexity of fine-tuning depend on the particular application. For example, in one study, a pre-trained CNN model designed for ECG analysis was fine-tuned to detect AF from PPG segments using a small set of labeled data. Another promising



technique is data augmentation to generate artificial samples to boost the number of samples for training the DL models and increasing the generalizability of model performance.

DL is the fastest growing approach of all three approaches for PPG-AF detection. We observe an average of 6 studies employing DL per year between 2019 and 2022, as compared to 3.5 studies/year between 2018 and 2019.

## 5. Discussion

While the performance metrics reported in Tables 2-4 suggest the promising potential of PPG for AF detection, several challenges remain. In this section, we will delve into these issues, offering insights drawn from our comprehensive analysis of the reviewed studies. Key concerns to be discussed include PPG signal quality, label accuracy, and the impact of concurrent arrhythmias. Studies that have considered these issues are summarized in Table 5. Furthermore, we extend our discussions to encompass additional considerations pertaining to PPG-based AF detection. These include algorithmic factors such as performance metrics, data sources, computational efficiency, domain shifts, as well as model explainability and equity.

Factors	Studies	Capacity	
Signal Quality	STAT	[16],[11],[17],[18],[26],[12],[27],[28],[13],[14],[15]	11/17
	ML	[29],[30],[31],[32],[33],[34],[35],[36],[37]	9/18
	DL	[38],[39],[40],[41],[42],[43],[44],[45],[46],[47],[48],[49]	12/24
Label Noise	STAT	[10],[28],[13],[15]	4/17
	ML	[30],[35],[50],[36]	4/18
	DL	[40],[51],[43],[47],[52],[48]	6/24
Concurrent Arrhythmias	STAT	[16],[17],[26],[27],[14]	5/17
	ML	[31],[36]	2/18
	DL	[40],[53],[48],[54]	4/24

**Table 5.** Challenging factors considered in the studies

### 5.1 PPG signal quality

PPG signal quality remains a considerable challenge, which is widely acknowledged within the scientific community. A multitude of complicating factors can compromise the PPG signal quality, including motion artifacts, skin tone variations, sensor pressure variations, respiratory cycles, and ambient light interference, only to name a few. The challenge of noise in PPG signal is particularly acute when it comes to the continuous acquisition of PPG, which is crucial for long-term monitoring of AF risk.

As reported in Table 5, most of the reviewed studies take signal quality into consideration, with 54% of the reviewed studies implementing measures to exclude PPG signals of poor quality. For example, in [27], the authors presented a noise artifact detection algorithm designed for detecting noise artifacts. Out of a total of 2,728 30-second PPG strips, only 314 strips were deemed suitable for further analysis after applying the algorithm. Similarly, in [41], the authors proposed a multi-tasking framework that incorporated both signal quality assessment and AF detection tasks. Only PPG signals of excellent quality were retained for the purpose of AF detection. This practice, however, harbors potential issues that warrant deeper consideration. Firstly, by systematically discarding vast swaths of signal data considered of inferior quality, the earliest possible detection of atrial fibrillation (AF) is inevitably delayed, creating a potentially significant time lag in diagnosis. Secondly, this approach harbors a statistical dilemma; the discarded PPG-AF signals could be construed as false positives within the context of the overall analysis. However, such instances are typically overlooked when calculating the positively predicted value or false positive rate, thereby potentially inflating the model's reported performance. Consequently, the reliance on selective data exclusion as a signal quality control strategy may inadvertently compromise the validity of the study's outcomes and the efficacy of predictive calculation would be based on the proportion of motion artifacts present within individual PPG segments, thus providing a more precise estimate of signal quality. Subsequently, an appropriate threshold could be ascertained to filter out PPG signals devoid of meaningful information. Alternatively, one can integrate the

signal quality information as part of the model input that controls the uncertainty level of the model output. These approaches would strike the balance of salvaging PPG signals with suboptimal quality for disrupt-less monitoring and model performance.

## **5.2 Label noise**

The issue of label noise in annotated datasets presents another significant challenge in the application of PPG for AF detection. Accurate and consistent labeling of datasets is crucial for the development and validation of reliable detection algorithms [56]. To achieve this, it usually involves more than two clinical domain experts to cross-check the agreement of annotations, and a reconciliation strategy needs to be in place in the event of disagreement. However, many studies often fall short in this aspect due to the labor-intensive task and an insufficient number of cardiologists available to annotate the datasets. Across the reviewed studies, only 9 out of the 59 studies [10, 13, 15, 28, 35, 36, 40, 47, 48] employed the expertise of at least two cardiologists for annotation, as reported in Table 5. This scarcity of expert annotators can result in imprecise and incomplete labeling of AF events, leading to label noise, which in turn, may undermine the performance of supervised learning algorithms.

Furthermore, the absence of standardized guidelines to address disagreements among annotators exacerbates this issue. In the event of conflicting annotations, the lack of a clear protocol or consensus mechanism can lead to inconsistencies in the dataset. This variability not only confounds the training of predictive models but also hampers the reproducibility of research findings. Consequently, establishing robust procedures for data annotation, which involve recruiting sufficient expert annotators and defining clear rules for resolving disagreements, is paramount. Addressing these issues would significantly enhance the quality of the annotated PPG datasets, thereby facilitating more reliable and accurate AF detection.

In addition to the shortage of expert involvement, the field faces another substantial challenge: the absence of clear clinical guidelines for annotating AF events using PPG data. Unlike ECG,

which has well-established guidelines for AF event labeling, PPG operates in a far less standardized environment. This lack of formalized guidance further exacerbates the risk of label noise, compromising both algorithmic performance and clinical reliability. Given these constraints, it becomes imperative to consider multimodal signal inputs when annotating data. Incorporating ECG or other established modalities alongside PPG can provide a more robust framework for annotation, thereby improving the quality of labeled data.

### **5.3 Concurrent arrhythmias**

The detection accuracy of AF through PPG can be significantly influenced by the presence of other arrhythmias, notably premature ventricular contractions (PVC) and premature atrial contractions (PAC). Both PVCs and PACs introduce irregularities into the heart rhythm that can mimic the rhythm irregularities seen in AF, potentially leading to false-positive detections. PVCs and PACs are characterized by early heartbeats originating from the ventricles and atria, respectively [27]. These early beats can disrupt the regular rhythm of the heart, resulting in PPG signal patterns that may resemble those associated with AF. Consequently, a PPG-based AF detection model might mistakenly classify these as AF events, thereby reducing the specificity of the model. Furthermore, the simultaneous presence of AF and other arrhythmias in the same patient adds another layer of complexity to the problem. This co-existence can modify the PPG signal's morphology in ways that differ from the signals of patients with AF or PVC/PAC alone, making it more difficult to accurately identify the presence of AF.

It is noteworthy that several studies considered the presence of arrhythmias other than AF, as shown in Table 5. For instance, in the study by [31, 36], the differentiation of PVC and PAC from AF using PPG signals was explored. The results of this investigation demonstrated successful differentiation between PVC/PAC and AF based on PPG signal characteristics. This finding suggests that PPG-based analysis holds promise for distinguishing various types of arrhythmias beyond AF. Thus, when developing and evaluating PPG-based AF detection models, it is critical

to account for the potential influence of other arrhythmias like PVC and PAC. Robust algorithms should be designed to discriminate between AF and these other rhythm disturbances to maintain high detection accuracy, reinforcing the necessity of comprehensive, diverse, and well-annotated training datasets in the development of these predictive models.

#### **5.4 Quantitative metrics for algorithm performance evaluation**

The studies reviewed in this work always use conventional performance metrics, such as the area under the receiver operational characteristics curve (AUROC), accuracy, sensitivity, specificity, and F1 Score. However, it's crucial to acknowledge that relying solely on these conventional metrics may be insufficient, particularly within the context of continuous health monitoring scenarios [57]. The landscape of continuous health monitoring, facilitated through wearable devices, unfolds as a dynamic and perpetually evolving terrain of data. Within this context, the intrinsic nature of a continuous data stream introduces complexities that transcend the conventional boundaries of traditional evaluation metrics. In scenarios wherein health-related parameters undergo ceaseless scrutiny, the spectrum of fluctuations, subtleties, and overarching trends assumes paramount significance. Conventional metrics, by design, tend to compartmentalize performance assessment within discrete segments, potentially missing the panoramic context that is intrinsic to continuous health monitoring. This paradigm invites us to reflect upon the necessity of embracing evaluation methodologies that are attuned to the temporal dynamics, such as assessing the frequency of AF occurrence that reflects AF burden, the nuances of variation, and the holistic import of trends.

#### **5.5 Domain shift problem**

models developed therefrom.

We propose a nuanced perspective on PPG signal quality assessment rather than adhering to the dichotomous approach of designating signals as merely black or white [7]. Instead, we suggest the computation of a Signal Quality Index (SQI) as a continuous metric [55]. This

PPG signals, despite their utility in non-invasive physiological monitoring, present certain complexities linked to the site of acquisition and inter-patient variability. It has been observed that PPG signals sourced from distinct anatomical sites yield diverse morphological patterns [58]. This is primarily due to the different vascular structures, skin thickness, and other physiological attributes specific to these sites. Such morphological variations can pose significant challenges in interpreting these signals and developing universally applicable models, as the distribution of signal characteristics is inherently contingent on the site of collection.

Moreover, inter-patient variability further compounds this issue by introducing additional variations in the data distribution. These variations stem from a wide array of factors, including demographic attributes (such as age and sex), physiological characteristics (including skin pigmentation and body mass index [BMI]), and medical conditions unique to individual patients [59]. For instance, an older patient might exhibit a different PPG signal morphology due to increased arterial stiffness, while individuals with darker skin might present a different signal-to-noise ratio owing to higher melanin content that can absorb more light than lighter skin.

These site-specific and inter-patient differences can induce what is referred to as a "domain shift" problem in machine learning [60, 61]. Here, a model that is trained on data from a specific group (for example, PPG signals from a certain body site or a particular patient group) may not generalize the model performance when it is applied to a different group. Therefore, while harnessing PPG signals for health monitoring and disease prediction, it is paramount to consider these variations and devise strategies to address the domain shift problem for reliable and generalized model performance.

## **5.6 Lack of large-scale labeled dataset**

In concert with the label noise issue discussed in Section 5.2, there exists a challenge of a paucity of large-scale, annotated datasets. To develop robust and reliable algorithms for AF detection, especially when deep learning models are employed, it requires extensive, labeled datasets. These ideal datasets should encompass a broad range of patient demographic groups, diverse health conditions, and various physiological states to ensure generalizable findings. Furthermore, they should contain precise annotations of the AF events in the PPG signal to facilitate effective supervised learning.

Emerging research is increasingly focused on addressing this issue by generating synthetic PPG signals through various data augmentation techniques. These range from traditional computational models that simulate physiologic PPG patterns (e.g., PPGSynth) [62] to advanced generative models such as Generative Adversarial Networks (GANs) [63, 64], Variational Autoencoders (VAEs) [65], and diffusion models. However, the extent to which these synthesized signals contribute to improved learning outcomes remains an open question. Recent research by Cheng et al. indicates the existence of a 'performance ceiling'—a limit to the improvements achieved by incorporating synthetic signals [64]. This underscores the need for further investigation into more effective algorithms for synthetic signal generation as well as a deeper understanding of this performance ceiling phenomenon.

To sum up, the lack of large, labeled datasets impedes the progress of research in this area, limiting the development and validation of predictive models. It restricts the ability to comprehensively evaluate and compare the performance of different AF detection methods under diverse and challenging conditions. Additionally, it hampers the exploration of more advanced machine learning techniques, which often necessitate large quantities of annotated data to train effectively. Therefore, efforts to collect/generate, share, and consolidate large-scale, well-annotated PPG datasets for AF detection represent a critical step to move the performance needle in this field.

## **5.7 Computational time**

With the rapid advancement of graphics processing units (GPUs) and increasing computational power, it is now feasible to train complex, large-scale neural networks that outperform traditional statistical or conventional machine learning methods [66]. However, this complexity presents new challenges, particularly for model inference. The inference process, which involves generating predictions from new data based on trained models, can be computationally demanding. This poses significant obstacles for wearable technologies that rely on edge computing, as these calculations can quickly deplete battery life, thereby undermining the feasibility of continuous monitoring [67]. Alternative solutions include offloading computational tasks to more powerful, tethered smartphones or to cloud-based platforms. Yet, both alternatives require robust and fast data streaming infrastructures.

Research efforts to address these challenges are bifurcated. On one hand, there is a burgeoning focus on 'tiny ML,' which aims to optimize neural network architectures for efficient edge computing without sacrificing performance. On the other hand, advancements in hardware and battery technology are driving the development of more powerful sensing techniques that enhance the capacity for long-term monitoring. Consequently, tackling these computational challenges necessitates orchestrated efforts from both research directions. It also underscores the imperative to keep computational requirements at the forefront when developing PPG-based AF detection algorithms.

## **5.8 Explainability**

Explainability in the context of PPG AF detection algorithms is a critical aspect that determines how well we understand the decision-making process of these algorithms. This is particularly important in healthcare, where the decisions made by these algorithms can have significant implications for patient care. Statistical methods are often considered naturally explainable because they rely on well-understood mathematical principles and procedures. For example, a



linear regression model, which lies in the intersection between statistical methods and machine learning, makes predictions based on a weighted sum of input features. The weights (or coefficients) assigned to each feature provide a direct measure of the feature's importance in the prediction, making it relatively straightforward to interpret the model's decisions. Machine learning methods, on the other hand, often involve more complex computations and may not be as directly interpretable as statistical methods. However, techniques have been developed to calculate feature importance, which can provide a certain level of explainability. For instance, in [68], the Fisher score method was employed to calculate the importance of features. The Fisher score is a statistical measure that evaluates the discriminative power of individual features in a classification task. By utilizing this method, the study aimed to assess the relevance and significance of different features in the context of atrial fibrillation detection. Similarly, in [37], each feature was input into the classifier separately, enabling the generation of a ranked list based on its impact on the overall classification performance through this sensitivity analysis.

Deep learning models, on the other hand, are often referred to as 'black boxes,' which make predictions based on intricate, high-dimensional mappings that are difficult to comprehend for humans. While they may achieve high predictive accuracy, it's often challenging to understand what features and their interactions the models use to make predictions, and how these features contribute to the final decision. This lack of transparency can be a major drawback in healthcare applications, where it's desirable to understand the underlying decision logic so as to gain trust from end users, such as clinicians and patients.

Several approaches are being explored to improve the explainability of deep learning models, including attention mechanisms, layer-wise relevance propagation, and model-agnostic methods like LIME (Local Interpretable Model-Agnostic Explanations) and SHAP (SHapley Additive exPlanations) [69-72]. A good example is [48], where authors used the guided gradient-weighted class activation mapping (Grad-CAM) approach to visualize crucial regions within the PPG signals

that enabled the model to predict a specific rhythm category. Despite these advances, explainability in deep learning remains an active area of research, particularly in the context of PPG-based AF detection.

### **5.9 Performance Bias and Model Equity**

Disparities in both access to and outcomes from utilizing digital health solutions and biotechnologies manifest a variety of identity dimensions, including economic status, social background, ethnicity, and gender [73]. As described by [74], health equity means, "...striving for the highest possible standard of health for all people and giving special attention to the needs of those at greatest risk of poor health, based on social conditions." In the context of PPG-based AF detection, this issue of equity extends across a spectrum of potential causes. It encompasses accessibility issues, particularly for individuals from rural areas or those with disadvantaged socioeconomic statuses, as well as physiological factors like skin tone and obesity, which can influence the reliability of PPG readings [75, 76]. Of the studies reviewed, a mere three explicitly touched upon the issue of performance bias and model equity [19, 45, 51]. This oversight underscores the pressing need to heighten awareness and equity considerations within the field. To tackle this challenge, a multidisciplinary approach is necessary, and healthcare providers, engineers, and researchers must proactively develop technologies that consider the needs of vulnerable and underrepresented populations.

## **6. Conclusion**

In conclusion, this comprehensive review highlights the growing significance of PPG-based AF detection in addressing a critical clinical challenge. The surge in research efforts, especially in machine learning and deep learning approaches, underscores the potential of PPG technology for continuous and accurate AF monitoring. While machine learning techniques offer versatility and promising results, deep learning models demonstrate remarkable performance by automating feature extraction. Nevertheless, challenges related to signal quality, label accuracy, and

concurrent arrhythmias persist, necessitating ongoing research and development. Furthermore, the availability of large-scale labeled datasets, computational efficiency, model explainability, and addressing performance bias and equity issues emerge as crucial considerations in advancing PPG-based AF detection technology. This review underscores the importance of continued collaboration between the medical and artificial intelligence communities to refine and deploy effective solutions for AF detection, ultimately improving patient outcomes in the face of this widespread health concern.

## Acknowledgment

This work was partially supported by NIH grant award R01HL166233.

## Reference

- [1] R. B. Schnabel *et al.*, “50 year trends in atrial fibrillation prevalence, incidence, risk factors, and mortality in the Framingham Heart Study: a cohort study,” *Lancet*, vol. 386, no. 9989, pp. 154-62, Jul. 2015. doi: 10.1016/s0140-6736(14)61774-8.
- [2] D. A. Lane, F. Skjøth, G. Y. H. Lip, T. B. Larsen, and D. Kotecha, “Temporal Trends in Incidence, Prevalence, and Mortality of Atrial Fibrillation in Primary Care,” *J. Am. Heart Assoc.*, vol. 6, no. 5, Apr. 2017. doi: 10.1161/jaha.116.005155.
- [3] N. Vinter, Q. Huang, M. Fenger-Grøn, L. Frost, E. J. Benjamin, and L. Trinquart, “Trends in excess mortality associated with atrial fibrillation over 45 years (Framingham Heart Study): community based cohort study,” *BMJ*, vol. 370, p. m2724, Aug. 2020. doi: 10.1136/bmj.m2724.
- [4] C. W. Tsao *et al.*, “Heart Disease and Stroke Statistics-2022 Update: A Report From the American Heart Association,” *Circulation*, vol. 145, no. 8, pp. e153-e639, Feb. 2022. doi: 10.1161/cir.0000000000001052.
- [5] A. Odutayo, C. X. Wong, A. J. Hsiao, S. Hopewell, D. G. Altman, and C. A. Emdin, “Atrial fibrillation and risks of cardiovascular disease, renal disease, and death: systematic review and meta-analysis,” *BMJ*, vol. 354, p. i4482, Sep. 2016. doi: 10.1136/bmj.i4482.
- [6] E. Lee *et al.*, “Mortality and causes of death in patients with atrial fibrillation: A nationwide population-based study,” *PLoS One*, vol. 13, no. 12, p. e0209687, Dec. 2018. doi: 10.1371/journal.pone.0209687.
- [7] P. H. Charlton *et al.*, “The 2023 wearable photoplethysmography roadmap,” *Physiol. Meas.*, Jul. 2023. doi: 10.1088/1361-6579/acead2.
- [8] T. Pereira *et al.*, “Photoplethysmography based atrial fibrillation detection: a review,” *NPJ Digit. Med.*, vol. 3, p. 3, Jan. 2020. doi: 10.1038/s41746-019-0207-9.

- [9] GitHub. (2023). *chengding0713 / Awesome-PPG-AF-detection*. Available: <https://github.com/chengding0713/Awesome-PPG-AF-detection>
- [10] E. S. Väliäho *et al.*, “Wrist band photoplethysmography in detection of individual pulses in atrial fibrillation and algorithm-based detection of atrial fibrillation,” *Europace*, vol. 21, no. 7, pp. 1031-1038, Jul. 2019. doi: 10.1093/europace/euz060.
- [11] T. Kabutoya *et al.*, “Diagnostic accuracy of an algorithm for detecting atrial fibrillation in a wrist-type pulse wave monitor,” *J. Clin. Hypertens. (Greenwich)*, vol. 21, no. 9, pp. 1393-1398, Sep. 2019. doi: 10.1111/jch.13648.
- [12] A. Sološenko, A. Petrėnas, B. Paliakaitė, L. Sörnmo, and V. Marozas, “Detection of atrial fibrillation using a wrist-worn device,” *Physiol. Meas.*, vol. 40, no. 2, p. 025003, Feb. 2019. doi: 10.1088/1361-6579/ab029c.
- [13] P. C. Chang, M. S. Wen, C. C. Chou, C. C. Wang, and K. C. Hung, “Atrial fibrillation detection using ambulatory smartwatch photoplethysmography and validation with simultaneous holter recording,” *Am. Heart J.*, vol. 247, pp. 55-62, May 2022. doi: 10.1016/j.ahj.2022.02.002.
- [14] D. Han *et al.*, “A Real-Time PPG Peak Detection Method for Accurate Determination of Heart Rate during Sinus Rhythm and Cardiac Arrhythmia,” *Biosensors (Basel)*, vol. 12, no. 2, Jan. 2022. doi: 10.3390/bios12020082.
- [15] E. S. Väliäho *et al.*, “Continuous 24-h Photoplethysmogram Monitoring Enables Detection of Atrial Fibrillation,” *Front. Physiol.*, vol. 12, p. 778775, Jan. 2021. doi: 10.3389/fphys.2021.778775.
- [16] L. M. Eerikäinen *et al.*, “How Accurately Can We Detect Atrial Fibrillation Using Photoplethysmography Data Measured in Daily Life?,” in *2019 Computing in Cardiology (CinC)*, Singapore, 2019, pp. 1-4. doi: 10.22489/CinC.2019.086.
- [17] S. K. Bashar *et al.*, “Atrial Fibrillation Detection from Wrist Photoplethysmography Signals Using Smartwatches,” *Sci. Rep.*, vol. 9, no. 1, p. 15054, Oct. 2019. doi: 10.1038/s41598-019-49092-2.
- [18] S. K. Bashar, D. Han, E. Ding, C. Whitcomb, D. D. McManus, and K. H. Chon, “Smartwatch Based Atrial Fibrillation Detection from Photoplethysmography Signals,” *Annu Int Conf IEEE Eng Med Biol Soc*, vol. 2019, pp. 4306-4309, Jul. 2019. doi: 10.1109/embc.2019.8856928.
- [19] R. Avram *et al.*, “Validation of an algorithm for continuous monitoring of atrial fibrillation using a consumer smartwatch,” *Heart Rhythm*, vol. 18, no. 9, pp. 1482-1490, Sep. 2021. doi: 10.1016/j.hrthm.2021.03.044.
- [20] N. M. Nonoguchi *et al.*, “Accuracy of wristwatch-type photoplethysmography in detecting atrial fibrillation in daily life(,)” *Eur. Heart J. Digit Health*, vol. 3, no. 3, pp. 455-464, Sep. 2022. doi: 10.1093/ehjdh/ztac041.
- [21] T. Chen and C. Guestrin, “XGBoost: A Scalable Tree Boosting System,” in *Proceedings of the 22nd ACM SIGKDD International Conference on Knowledge Discovery and Data Mining*, San Francisco, California, USA, 2016, pp. 785–794. doi: 10.1145/2939672.2939785.

- [22] C. Cortes and V. Vapnik, "Support-vector networks," *Mach. Lear.*, vol. 20, pp. 273-297, Sept. 1995. doi: 10.1007/BF00994018.
- [23] Y. Shen, M. Voisin, A. Aliamiri, A. Avati, A. Hannun, and A. Ng, "Ambulatory Atrial Fibrillation Monitoring Using Wearable Photoplethysmography with Deep Learning," in *Proceedings of the 25th ACM SIGKDD International Conference on Knowledge Discovery & Data Mining*, Anchorage, AK, USA, 2019, pp. 1909–1916. doi: 10.1145/3292500.3330657.
- [24] K. He, X. Zhang, S. Ren, and J. Sun. (2015, 15 October 2023). *Deep residual learning for image recognition*. Available: <http://image-net.org/challenges/LSVRC/2015/>
- [25] S. Hochreiter and J. Schmidhuber, "Long short-term memory," *Neural Comput.*, vol. 9, no. 8, pp. 1735-80, Nov. 1997. doi: 10.1162/neco.1997.9.8.1735.
- [26] D. Han *et al.*, "Smartwatch PPG Peak Detection Method for Sinus Rhythm and Cardiac Arrhythmia," *Annu. Int. Conf. IEEE Eng. Med. Biol. Soc.*, vol. 2019, pp. 4310-4313, Jul. 2019. doi: 10.1109/embc.2019.8857325.
- [27] D. Han *et al.*, "Premature Atrial and Ventricular Contraction Detection using Photoplethysmographic Data from a Smartwatch," *Sensors (Basel)*, vol. 20, no. 19, Oct. 2020. doi: 10.3390/s20195683.
- [28] E. S. Väliäho *et al.*, "Wrist Band Photoplethysmography Autocorrelation Analysis Enables Detection of Atrial Fibrillation Without Pulse Detection," *Front Physiol*, vol. 12, p. 654555, May 2021. doi: 10.3389/fphys.2021.654555.
- [29] Neha, R. Kanawade, S. Tewary, and H. K. Sardana, "Photoplethysmography Based Arrhythmia Detection and Classification," in *2019 6th International Conference on Signal Processing and Integrated Networks (SPIN)*, Noida, India, 2019, pp. 944-948. doi: 10.1109/SPIN.2019.8711737.
- [30] S. Fallet, M. Lemay, P. Renevey, C. Leupi, E. Pruvot, and J. M. Vesin, "Can one detect atrial fibrillation using a wrist-type photoplethysmographic device?," *Med Biol Eng Comput*, vol. 57, no. 2, pp. 477-487, Feb. 2019. doi: 10.1007/s11517-018-1886-0.
- [31] L. M. Eerikainen *et al.*, "Detecting Atrial Fibrillation and Atrial Flutter in Daily Life Using Photoplethysmography Data," *IEEE J. Biomed. Health Inform.*, vol. 24, no. 6, pp. 1610-1618, Jun. 2020. doi: 10.1109/jbhi.2019.2950574.
- [32] D. Mol *et al.*, "Performance of an automated photoplethysmography-based artificial intelligence algorithm to detect atrial fibrillation," *Cardiovasc. Digit. Health J.*, vol. 1, no. 2, pp. 107-110, Sep-Oct 2020. doi: 10.1016/j.cvdhj.2020.08.004.
- [33] Y. Guo *et al.*, "Photoplethysmography-Based Machine Learning Approaches for Atrial Fibrillation Prediction: A Report From the Huawei Heart Study," *JACC Asia*, vol. 1, no. 3, pp. 399-408, Dec. 2021. doi: 10.1016/j.jacasi.2021.09.004.
- [34] Neha, H. K. Sardana, R. Kanawade, and N. Dogra, "Photoplethysmograph based arrhythmia detection using morphological features," *Biomedical Signal Processing and Control*, vol. 81, p. 104422, Mar. 2023. doi: 10.1016/j.bspc.2022.104422.

- [35] L. Zhu *et al.*, "Atrial Fibrillation Detection and Atrial Fibrillation Burden Estimation via Wearables," *IEEE J. Biomed. Health Inform.*, vol. 26, no. 5, pp. 2063-2074, May 2022. doi: 10.1109/jbhi.2021.3131984.
- [36] M. T. Liao *et al.*, "Impact of recording length and other arrhythmias on atrial fibrillation detection from wrist photoplethysmogram using smartwatches," *Sci. Rep.*, vol. 12, no. 1, p. 5364, Mar. 2022. doi: 10.1038/s41598-022-09181-1.
- [37] L. Jeanningros *et al.*, "Pulse Wave Analysis of Photoplethysmography Signals to Enhance Classification of Cardiac Arrhythmias," in *2022 Computing in Cardiology (CinC)*, Tampere, Finland, 2022, vol. 498, pp. 1-4. doi: 10.22489/CinC.2022.023.
- [38] Z. Rezaei Yousefi *et al.*, "Atrial Fibrillation Detection from Wrist Photoplethysmography Data Using Artificial Neural Networks," in *World Congress on Medical Physics and Biomedical Engineering 2018*, Singapore, 2019, pp. 399-404. doi: 10.1007/978-981-10-9038-7\_75.
- [39] J. V. Zaen *et al.*, "Atrial Fibrillation Detection from PPG Interbeat Intervals via a Recurrent Neural Network," in *2019 Computing in Cardiology (CinC)*, Singapore, 2019, pp. Page 1-Page 4. doi: 10.22489/CinC.2019.084.
- [40] S. Kwon *et al.*, "Deep Learning Approaches to Detect Atrial Fibrillation Using Photoplethysmographic Signals: Algorithms Development Study," *JMIR Mhealth Uhealth*, vol. 7, no. 6, p. e12770, Jun. 2019. doi: 10.2196/12770.
- [41] J. Torres-Soto and E. A. Ashley, "Multi-task deep learning for cardiac rhythm detection in wearable devices," *NPJ Digit. Med.*, vol. 3, p. 116, 2020. doi: 10.1038/s41746-020-00320-4.
- [42] J. L. Selder *et al.*, "Assessment of a standalone photoplethysmography (PPG) algorithm for detection of atrial fibrillation on wristband-derived data," *Comput. Methods Programs Biomed.*, vol. 197, p. 105753, Dec. 2020. doi: 10.1016/j.cmpb.2020.105753.
- [43] S. Kwon *et al.*, "Detection of Atrial Fibrillation Using a Ring-Type Wearable Device (CardioTracker) and Deep Learning Analysis of Photoplethysmography Signals: Prospective Observational Proof-of-Concept Study," *J. Med. Internet Res.*, vol. 22, no. 5, p. e16443, May 21 2020. doi: 10.2196/16443.
- [44] E. Chen *et al.*, "A new smart wristband equipped with an artificial intelligence algorithm to detect atrial fibrillation," *Heart Rhythm*, vol. 17, no. 5 Pt B, pp. 847-853, May 2020. doi: 10.1016/j.hrthm.2020.01.034.
- [45] H. Zhang *et al.*, "Towards Early Detection and Burden Estimation of Atrial Fibrillation in an Ambulatory Free-living Environment," *J Proc. ACM Interact. Mob. Wearable Ubiquitous Technol.*, vol. 5, no. 2, pp. 1–19, Jun. 2021. doi: 10.1145/3463503.
- [46] S. S. S. Das *et al.*, "BayesBeat: Reliable Atrial Fibrillation Detection from Noisy Photoplethysmography Data," *Proc. ACM Interact. Mob. Wearable Ubiquitous Technol.*, vol. 6, no. 1, pp. 1–21, Mar. 2022. doi: 10.1145/3517247.
- [47] D. H. Nguyen, P. C. P. Chao, C. C. Chung, R. H. Horng, and B. Choubey, "Detecting Atrial Fibrillation in Real Time Based on PPG via Two CNNs for Quality Assessment and Detection," *IEEE Sensors J.*, vol. 22, no. 24, pp. 24102-24111, Dec. 2022. doi: 10.1109/JSEN.2022.3217037.

- [48] Z. Liu *et al.*, "Multiclass Arrhythmia Detection and Classification From Photoplethysmography Signals Using a Deep Convolutional Neural Network," *J. Am. Heart Assoc.*, vol. 11, no. 7, p. e023555, Apr. 2022. doi: 10.1161/jaha.121.023555.
- [49] Neha, H. K. Sardana, N. Dogra, and R. Kanawade, "Dynamic time warping based arrhythmia detection using photoplethysmography signals," *Signal, Image and Video Processing*, vol. 16, no. 7, pp. 1925-1933, Jan. 2022. doi: 10.1007/s11760-022-02152-z.
- [50] D. Hiraoka *et al.*, "Diagnosis of Atrial Fibrillation Using Machine Learning With Wearable Devices After Cardiac Surgery: Algorithm Development Study," *JMIR Form. Res.*, vol. 6, no. 8, p. e35396, Aug. 2022. doi: 10.2196/35396.
- [51] K. Aschbacher *et al.*, "Atrial fibrillation detection from raw photoplethysmography waveforms: A deep learning application," *Heart Rhythm O2*, vol. 1, no. 1, pp. 3-9, Apr. 2020. doi: 10.1016/j.hroo.2020.02.002.
- [52] S. Kwon *et al.*, "Atrial fibrillation detection in ambulatory patients using a smart ring powered by deep learning analysis of continuous photoplethysmography monitoring," *Eur. Heart J.*, vol. 43, no. S2, p. ehac544.415, Oct. 2022. doi: 10.1093/eurheartj/ehac544.415.
- [53] E. Genzoni *et al.*, "Challenging the Limitations of Atrial Fibrillation Detection in the Presence of Other Cardiac Arrhythmias," *Annu. Int. Conf. IEEE Eng. Med. Biol. Soc.*, vol. 2020, pp. 5000-5003, Jul. 2020. doi: 10.1109/embc44109.2020.9176418.
- [54] C. Ding, Z. Guo, A. Shah, G. Clifford, C. Rudin, and X. Hu, "Cluster consistency: Simple yet effect robust learning algorithm on large-scale photoplethysmography for atrial fibrillation detection in the presence of real-world label noise," *arXiv preprint arXiv:2211.03333*, Nov. 2022. doi: 10.48550/arXiv.2211.03333.
- [55] Z. Guo, C. Ding, X. Hu, and C. Rudin, "A supervised machine learning semantic segmentation approach for detecting artifacts in plethysmography signals from wearables," *Physiol. Meas.*, vol. 42, no. 12, Dec. 2021. doi: 10.1088/1361-6579/ac3b3d.
- [56] H. Song, M. Kim, D. Park, Y. Shin, and J. G. Lee, "Learning From Noisy Labels With Deep Neural Networks: A Survey," *IEEE Trans. Neural Netw. Learn. Syst.*, Mar. 2022. doi: 10.1109/tnnls.2022.3152527.
- [57] M. Butkuvienė, A. Petrenas, A. Solosenko, A. Martin-Yebra, V. Marozas, and L. Sornmo, "Considerations on Performance Evaluation of Atrial Fibrillation Detectors," *IEEE Trans. Biomed. Eng.*, vol. 68, no. 11, pp. 3250-3260, Nov. 2021. doi: 10.1109/tbme.2021.3067698.
- [58] V. Fleischhauer, J. Bruhn, S. Rasche, and S. Zaunseder, "Photoplethysmography upon cold stress-impact of measurement site and acquisition mode," *Front. Physiol.*, vol. 14, p. 1127624, Jun. 2023. doi: 10.3389/fphys.2023.1127624.
- [59] D. Clifton, J. G. Douglas, P. S. Addison, and J. N. Watson, "Measurement of respiratory rate from the photoplethysmogram in chest clinic patients," *J. Clin. Monit. Comput.*, vol. 21, no. 1, pp. 55-61, Feb. 2007. doi: 10.1007/s10877-006-9059-3.
- [60] M. Radha *et al.*, "A deep transfer learning approach for wearable sleep stage classification with photoplethysmography," *NPJ Digit. Med.*, vol. 4, no. 1, p. 135, Sept. 2021. doi: 10.1038/s41746-021-00510-8.

- [61] M. Wang and W. Deng, "Deep visual domain adaptation: A survey," *Neurocomputing*, vol. 312, pp. 135-153, Oct. 2018. doi: 10.1016/j.neucom.2018.05.083.
- [62] Q. Tang *et al.*, "PPGSynth: An Innovative Toolbox for Synthesizing Regular and Irregular Photoplethysmography Waveforms," *Front. Med. (Lausanne)*, vol. 7, p. 597774, Nov. 2020. doi: 10.3389/fmed.2020.597774.
- [63] I. Goodfellow *et al.*, "Generative adversarial networks," *Commun. ACM*, vol. 63, no. 11, pp. 139-144, Oct. 2020. doi: 10.1145/3422622.
- [64] C. Ding *et al.*, "Log-Spectral Matching GAN: PPG-based Atrial Fibrillation Detection can be Enhanced by GAN-based Data Augmentation with Integration of Spectral Loss," *IEEE J. Biomed. Health Inform.*, vol. 27, no. 3, pp. 1331-1341, Jan. 2023. doi: 10.1109/jbhi.2023.3234557.
- [65] D. P. Kingma and M. Welling, "Auto-encoding variational bayes," *arXiv preprint arXiv:1312.6114*, Dec. 2013. doi: 10.48550/arXiv.1312.6114.
- [66] N. C. Thompson, K. Greenewald, K. Lee, and G. F. Manso, "The computational limits of deep learning," *arXiv preprint arXiv:2007.05558*, Jul. 2020. doi: 10.48550/arXiv.2007.05558.
- [67] J. Chen and X. Ran, "Deep Learning With Edge Computing: A Review," *Proceedings of the IEEE*, vol. 107, no. 8, pp. 1655-1674, Jul. 2019. doi: 10.1109/JPROC.2019.2921977.
- [68] C. Yang, C. Veiga, J. J. Rodríguez-Andina, J. Fariña, A. Iñiguez, and S. Yin, "Using PPG Signals and Wearable Devices for Atrial Fibrillation Screening," *IEEE Trans. Ind. Electr.*, vol. 66, no. 11, pp. 8832-8842, 2019. doi: 10.1109/TIE.2018.2889614.
- [69] B. Zhou, A. Khosla, A. Lapedriza, A. Oliva, and A. Torralba, "Learning Deep Features for Discriminative Localization," in *2016 IEEE Conf. Computer Vision and Pattern Recognition (CVPR)*, Las Vegas, NV, USA, 2016, pp. 2921-2929. doi: 10.1109/CVPR.2016.319.
- [70] A. Binder, G. Montavon, S. Lapuschkin, K.-R. Müller, and W. Samek, "Layer-Wise Relevance Propagation for Neural Networks with Local Renormalization Layers," in *Artificial Neural Networks and Machine Learning—ICANN 2016*, Cham, 2016, pp. 63-71. doi: 10.1007/978-3-319-31720-7\_4.
- [71] M. T. Ribeiro, S. Singh, and C. Guestrin, "'Why Should I Trust You?': Explaining the Predictions of Any Classifier," in *Proceedings of the 22nd ACM SIGKDD International Conference on Knowledge Discovery and Data Mining*, San Francisco, California, USA, 2016, pp. 1135–1144. doi: 10.1145/2939672.2939778.
- [72] S. M. Lundberg and S.-I. Lee, "A unified approach to interpreting model predictions," in *Proceedings of the 31st International Conference on Neural Information Processing Systems*, Long Beach, California, USA, 2017, pp. 4768–4777.
- [73] O. L. Lanier, M. D. Green, G. A. Barabino, and E. Cosgriff-Hernandez, "Ten simple rules in biomedical engineering to improve healthcare equity," *PLoS Comput. Biol.*, vol. 18, no. 10, p. e1010525, Oct. 2022. doi: 10.1371/journal.pcbi.1010525.
- [74] P. Braveman, "What are health disparities and health equity? We need to be clear," *Public Health Rep.*, vol. 129, no. S2, pp. 5-8, Jan-Feb 2014. doi: 10.1177/00333549141291s203.



- [75] J. Fine *et al.*, "Sources of Inaccuracy in Photoplethysmography for Continuous Cardiovascular Monitoring," *Biosensors (Basel)*, vol. 11, no. 4, Apr. 2021. doi: 10.3390/bios11040126.
- [76] Ajmal, T. Boonya-Ananta, A. J. Rodriguez, V. N. Du Le, and J. C. Ramella-Roman, "Monte Carlo analysis of optical heart rate sensors in commercial wearables: the effect of skin tone and obesity on the photoplethysmography (PPG) signal," *Biomed. Opt. Express*, vol. 12, no. 12, pp. 7445-7457, Dec. 2021. doi: 10.1364/boe.439893.